De Novo Variants in *CDK19* Are Associated with a Syndrome Involving Intellectual Disability and Epileptic Encephalopathy

Hyung-lok Chung,[1,2,3,11] Xiao Mao,[4,5,11] Hua Wang,[4,5] Ye-Jin Park,[1] Paul C. Marcogliese,[1,2] Jill A. Rosenfeld,[1] Lindsay C. Burrage,[1] Pengfei Liu,[1,6] David R. Murdock,[1] Shinya Yamamoto,[1,2] Michael F. Wangler,[1,2] Undiagnosed Diseases Network, Hsiao-Tuan Chao,[1,2,7,8,9] Hongyu Long,[10] Li Feng,[10] Carlos A. Bacino,[1] Hugo J. Bellen,[1,2,3,*] and Bo Xiao[10,*]

We identified three unrelated individuals with *de novo* missense variants in *CDK19*, encoding a cyclin-dependent kinase protein family member that predominantly regulates gene transcription. These individuals presented with hypotonia, global developmental delay, epileptic encephalopathy, and dysmorphic features. CDK19 is conserved between vertebrate and invertebrate model organisms, but currently abnormalities in *CDK19* are not known to be associated with a human disorder. Loss of *Cdk8*, the fly homolog of *CDK19*, causes larval lethality, which is suppressed by expression of human *CDK19* reference cDNA. In contrast, the CDK19 p.Tyr32His and p.Thr196Ala variants identified in the affected individuals fail to rescue the loss of *Cdk8* and behave as null alleles. Additionally, neuronal RNAi-mediated knockdown of *Cdk8* in flies results in semi-lethality. The few eclosing flies exhibit severe seizures and a reduced lifespan. Both phenotypes are fully suppressed by moderate expression of the *CDK19* reference cDNA but not by expression of the two variants. Finally, loss of *Cdk8* causes an obvious loss of boutons and synapses at larval neuromuscular junctions (NMJs). Together, our findings demonstrate that human CDK19 fully replaces the function of Cdk8 in the fly, the human disease-associated *CDK19* variants behave as strong loss-of-function variants, and deleterious *CDK19* variants underlie a syndromic neurodevelopmental disorder.

Infantile spasms are caused by dysfunction of the developing nervous system and begin in the first 2 years of life, most commonly between 4 and 8 months of age.[1] Infantile spasms are a symptom of generalized brain disturbance and can be caused by infection,[2] developmental brain abnormalities,[3] or genetic disorders such as Down syndrome (MIM: 190685), tuberous sclerosis (MIM: 191100),[4] *ARX*-related disorders (MIM: 300419), and *CDKL5* pathogenic variants (MIM: 300672).[5] Much progress has been made in the past few years in the identification of genes responsible for infantile spasms, but for many the overall prognosis is poor.[6]

Cyclin-dependent kinase 19 (CDK19 [MIM: 614720]) and its paralog, CDK8 (MIM: 603184), are members of the transcriptional CDKs. Unlike other CDKs, these transcriptional CDKs are less involved in cell-cycle regulatory processes and are more involved in transcription.[7] CDK19 and CDK8 both interact with cyclin C (MIM: 123838) and mediators. CDK19 forms a CDK module by interacting with MED12L (MIM: 611318) and MED13L (MIM: 608771), whereas CDK8 does so by interacting with MED12 (MIM: 300188) and MED13 (MIM: 603808).[8] Note that MED13L and MED12 are known disease genes associated with intellectual disability.[9,10] This CDK module interacts with the core mediators to regulate RNA polymerase II to control transcriptional activity. *CDK8* has been a focus of some studies because it has been implicated in a number of important pathways, including those involving WNT signaling, KRAS, and Notch in cancers.[11,12] In contrast, much less is known about *CDK19*.

Initially, CDK19 was thought to function similarly or redundantly to CDK8 given that they share 84% amino acid sequence similarity and 97% identity in the kinase domain.[13] However, significant functional differences have been uncovered. Recently, *in vitro* studies have shown that CDK19 and CDK8 participate in mutually exclusive complexes,[14] and knockdown studies in cell lines of cervical cancer[7] and colon cancer[14] showed that they regulate the expression of different genes. Overall, CDK19 appears to have more specialized roles than CDK8. It is worth noting that complete loss of *Cdk8* is lethal in mice,[15] whereas complete loss of *Cdk19* is viable.[16] However, neurologic phenotypes have not yet been reported with homozygous loss of *Cdk19*.

Through collaboration with the Undiagnosed Diseases Network (UDN) and Xiangya Hospital in China, we identified three individuals who came from three independent families and have *de novo* missense *CDK19* variants.

[1]Department of Molecular and Human Genetics, Baylor College of Medicine, Houston, TX 77030, USA; [2]Jan and Dan Duncan Neurological Research Institute, Texas Children's Hospital, Houston, TX 77030, USA; [3]Howard Hughes Medical Institute, Baylor College of Medicine, Houston, TX 77030, USA; [4]National Health Commission Key Laboratory of Birth Defects Research, Prevention, and Treatment, Hunan Provincial Maternal and Child Health Care Hospital, Changsha 410008, China; [5]Department of Medical Genetics, Maternal and Child Health Hospital of Hunan Province, Changsha, Hunan 410008, China; [6]Baylor Genetics, Houston, TX 22021, USA; [7]Department of Pediatrics, Division of Neurology and Developmental Neuroscience, Baylor College of Medicine, Houston, TX 77030, USA; [8]Department of Neuroscience, Baylor College of Medicine, Houston, TX 77030, USA; [9]McNair Medical Institute, The Robert and Janice McNair Foundation, Houston, TX 77030, USA; [10]Neurology Department, Xiangya Hospital, Central South University, Changsha, Hunan 410008, China
[11]These authors contributed euqally to this work.
*Correspondence: hbellen@bcm.edu (H.J.B.), xiaobo_xy@126.com (B.X.)
https://doi.org/10.1016/j.ajhg.2020.04.001.

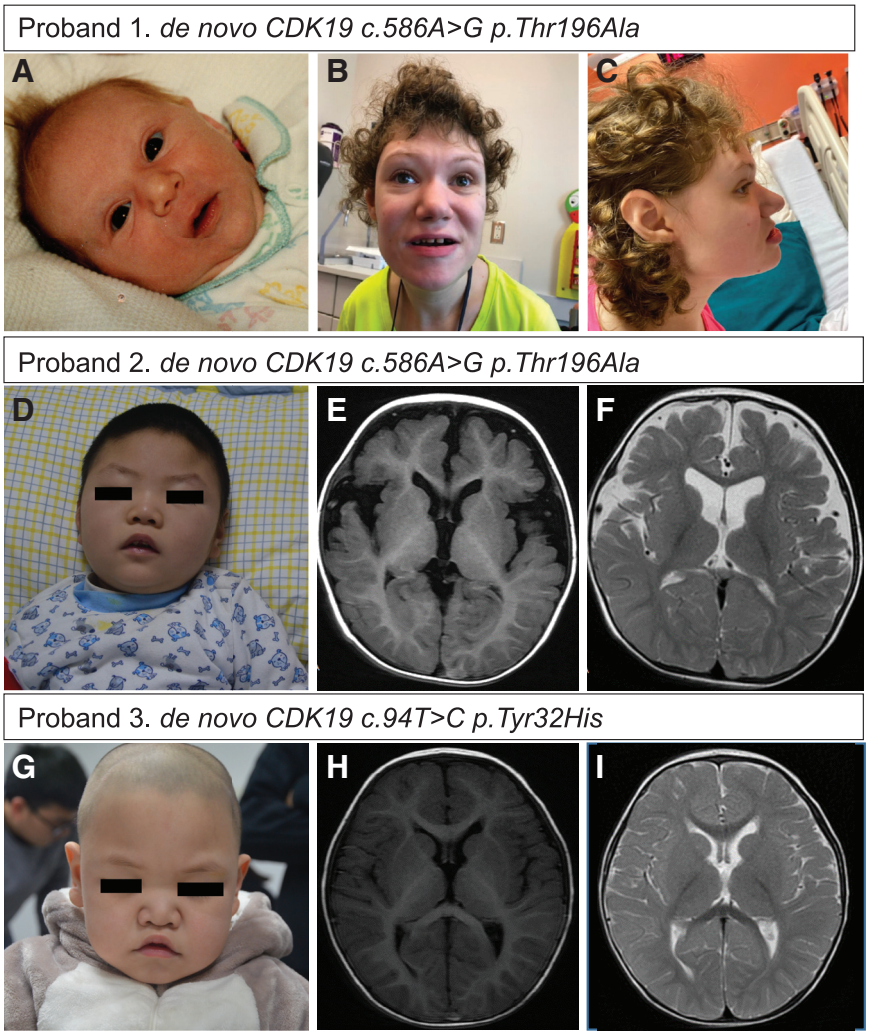

Figure 1. Clinical Features of Probands
(A) Front view of proband 1 at age 21 years. Distinctive features include thin, sparse, arched eyebrows; curly hair; mild hypotelorism; a prominent bulbous nose; a wide mouth with wide spaced teeth; a thin upper lip; and a long smooth philtrum.
(B) Facial profile of proband 1 at age 23 years shows midface retrusion.
(C) Photograph of proband 1 from the newborn period shows mild hypotelorism and fleshy nose.
(D) Dysmorphic facial features, including hypotelorism and a prominent nose with a bulbous tip, were observed in proband 2.
(E and F) T1 (E) and T2 (F) brain MRI images for proband 2 show mild atrophy.
(G) Dysmorphic features, including ocular hypertelorism; a prominent nose with a bulbous tip,;U-shaped vermillion and arched upper lip; and a large mouth were observed in proband 3.
(H and I) T1 (H) and T2 (I) brain MRI images for proband 3 show delayed myelination.

Proband 1 was a participant in the UDN study at Baylor College of Medicine. Probands 2 and 3 were each recruited to the Xiangya hospital Epilepsy Cohort, which aims to elucidate the genetic basis of epilepsy and epilepsy-related neurodevelopmental disorders. Probands 2 and 3 were recruited to the study during 2018 and 2019. Both of them underwent detailed medical-history collection and physical examination by neurologists. Informed consent for the diagnostic and research studies and publication including photos was obtained for all subjects (see Supplemental Information). Proband 1 is currently a 25-year-old female with a long-standing history of severe developmental delay and intellectual disability. She was born after a full-term pregnancy to non-consanguineous parents. Dysmorphic facial features were noted at birth (Figure 1A and Table 1). She presented at 4 months of age with poor head growth and delayed developmental milestones. She crawled and sat at 9 months and spoke three words by 12–15 months. At 15 months of age, she developed generalized tonic-clonic seizures that were refractory to multiple anti-epileptic medications and led to neurologic regression with loss of speech. She walked at 5 years of age with the help of orthotics. In addition, she has significant joint laxity resulting in many joint dislocations and a history of severe pica. Her clinical features, including hypotonia, ataxia, mouthing behaviors, constipation, seizures, hand flapping, and absent speech, were considered to be similar to those of Angelman syndrome (MIM: 105830), but genetic testing for that syndrome was negative. Her physical exam at 25 years old showed dysmorphic features such as hypotelorism, straight eyebrows, a prominent nose with a bulbous tip, midface hypoplasia, and a large mouth with widely spaced teeth (Figures 1A–1C). Her height was 159.5 cm (37^{th} percentile), her weight was 55.7 kg (30^{th} percentile), and her head circumference was 52.5 cm (5^{th} percentile). She has mild scoliosis. Her neurological exam was notable for acquired microcephaly, absent speech, diffuse hypotonia, symmetrically reduced reflexes, raking grasp, and a wide-based gait with an inverted and inward-turned left foot. She continues to have a generalized tonic-clonic seizure every 2–3 weeks, weekly complex partial seizures described as episodes of eye fluttering and eye dilation with altered consciousness, and a few nocturnal seizures per week. Current antiepileptic medications include daily valproic acid and clonazepam as needed. Her seizures had previously responded well to a ketogenic diet. Prior genetic testing included normal chromosome analysis (46, XX); normal Angelman methylation studies; normal sequencing of *UBE3A* (MIM: 601623); *FOXG1* (MIM: 164874), *CDKL5*, and *MECP2* (MIM: 300005) sequencing including deletion and duplication studies; and a normal chromosomal microarray. A repeat chromosomal microarray with SNP analysis

Table 1. Clinical Features of Affected Individuals with *De Novo CDK19* Variants

Proband	Proband 1	Proband 2	Proband 3
CDK19 variant	*de novo*, c.586A>G (p.Thr196Ala)	*de novo*, c.586A > G (p.Thr196Ala)	*de novo*, c.94T > C (p.Tyr32His)
Sex	female	male	male
Age	25 years	2 years	1 year
Global developmental delay	yes	yes	yes
Epilepsy	yes	yes/infantile spasms	yes/infantile spasms
Hypotonia	yes	yes	yes
Intellectual disability	yes	not applicable	not applicable
Dysmorphic features	yes	yes	yes
Scoliosis	yes	no	no
Brain MRI	borderline microcephaly	mild atrophy	delayed myelination
Other findings	autism, ataxia, short stature	not applicable	small calculus at both kidneys

revealed a benign small duplication on 5p. In addition, she had a clinical proband exome sequencing (ES) that revealed only heterozygous variants of uncertain significance in genes associated with autosomal disorders, which were all inherited from an unaffected parent. Thus, she was referred to the UDN for further evaluation and received trio whole-genome sequencing (WGS). A *de novo* coding variant was identified in *CDK19* (Genbank: NM_015076.4, exon 6, c.586A>G[p.Thr196Ala]) and confirmed by Sanger sequencing (Table 1).

Proband 2 is a 2-year-old male. He was born after a normal 38-week gestation to non-consanguineous parents. At 10 weeks of age, he developed episodes of cyanosis. At 6 months of age, he developed generalized tonic-clonic seizures. 1 month later, the individual developed infantile spasms occurring in clusters dozens of times per day. Electroencephalogram (EEG) showed hypsarrhythmia with burst suppression. Parenteral adrenocorticotropic hormone (ACTH) injections and oral antiepileptic drugs, including sodium valproate and topiramate, failed to control the seizures. A ketogenic diet was tried but did not help to control seizures. At 16 months of age, levetiracetam was added but was ineffective. Currently, a combination of sodium valproate, topiramate, and lamotrigine are being used. The individual has delay in developmental milestones. At present, he is able to lift his head, although barely, but is unable to track objects, roll, sit, or crawl. He does not babble. MRI brain findings showed mild brain atrophy (Figures 1E and 1F), and neurological examination showed diffuse hypotonia. His dysmorphic facial features include hypotelorism, a prominent nose with a bulbous tip, and a large mouth with widely spaced teeth (Figure 1D and Table 1). His height is 86 cm (28th percentile), his weight is 11.5 kg (32th percentile), and his head circumference is 47.5 cm (29th percentile). Clinical ES and SNP array (for copy number variants) were performed, but no pathogenic variants were identified (see Supplemental Information). A trio-ES identified a *de novo* coding variant in *CDK19* (GenBank: NM_015076.4, exon 6, c.586A>G [p.Thr196Ala]). Sanger sequencing confirmed the result.

Proband 3 is an 18-month-old male. He was born at 39 weeks' gestation to non-consanguineous parents. No abnormalities were identified at birth or at his 1 month evaluation. Developmentally, he was unable to hold his head at 6 months of age. He could sit without support at 12 months of age but could not crawl until the latest evaluation at 18 months old. His brain MRI showed delayed myelination (Figures 1H and 1I), and a neurologic exam was significant for diffuse hypotonia (Table 1). At 9 months of age, he developed daily atonic seizures. EEG studies revealed hypsarrhythmia. After he was given ACTH for 1 week, the drug was stopped because of a concomitant infection and immunosuppression concerns. Since then, various antiepileptic drugs have been used and have been unable to control the seizures. Recent examination findings were significant for dysmorphic features, including ocular hypertelorism, a prominent nose with a bulbous tip, a highly arched palate, U-shape vermillion of the upper lip, a large mouth with widely spaced teeth, an arched upper lip, and a single transverse palmar crease in his right hand (Figure 1G and Table 1). His height is 90 cm (99.8th percentile), his weight is 15.5 kg (99.9th percentile), and his head circumference 48 cm (67.9th percentile). Target gene-panel analysis was performed, but no pathogenic variants were found (Supplemental Information). Trio-ES was performed, and a *de novo* variant was identified (*CDK19*, GenBank: NM_015076.3, exon 1, c.94T>C [p.Tyr32His]). Sanger sequencing validated the variant.

Neither *CDK19* variant (neither p.Tyr32His identified in proband 3 nor p.Thr196Ala identified in probands 1 and 2) is present in control population databases such as gnomAD.[17] The pLI score of *CDK19* is 1, which indicates a high probability of intolerance to loss of function, and

Table 2. The Pathogenicity of Two *De Novo CDK19* Variants

Genomic position (hg19)	6:111136246	6:110953293
Variant (*de novo*)	GenBank: NM_015076.3: c.586A>G	GenBank: NM_015076.3: c.94T>C
Amino Acid change	p.Thr196Ala	p.Tyr32His
CADD	26.6	27.8
SIFT	0.001 damaging	0.000 damaging
PolyPhen2 HDIV	0.999 probably damaging	1.000 probably damaging
PolyPhen2 HVAR	0.995 probably damaging	0.995 probably damaging
LRT	0.000 deleterious	0.000 deleterious
Mutation Taster	1 disease causing	1 disease causing
PROVEAN	−4.53 damaging	−4.27 damaging
M-CAP	0.113 damaging	0.178 damaging

the missense *Z* score of *CDK19* is 3.56, indicating that the gene is also intolerant to missense variation. Furthermore, variant pathogenicity prediction through several tools strongly indicates that these variants are likely pathogenic (Table 2).

The sole homolog of *CDK19* in the fly is *Cdk8*. The human genome carries two homologs of *Cdk8* (*CDK8* and *CDK19*). Overall, fly Cdk8 and CDK19 share 75% similarity and 68% identity.[18,19] The serine-threonine kinase domain that phosphorylates the mediator complex to control transcription[13] is very well conserved, with 99% homology (Figure 2A).

We first generated UAS-transgenic flies with the *CDK19* variants p.Tyr32His and p.Thr196Ala, as well as the reference *CDK19* cDNA. To examine whether there are any functional differences between the reference *CDK19* and variants, we ubiquitously overexpressed *CDK19* cDNAs by using a strong ubiquitous driver, tubulin Gal4 (Tub-Gal4), in a wild-type background. Expression of the reference *CDK19* does not affect viability, but the variants caused a decrease in viability to 69% (CDK19, p.Tyr32His) or 53% (CDK19, p.Thr196Ala). Hence, the variants function differently *in vivo* than does the reference, and our data suggest that these variants are most likely dominant mutations (Figure 2B).

To determine whether the reference *CDK19* or variants can replace the loss of function of *Cdk8*, we performed rescue experiments with a $Cdk8^{K185}$ null allele.[20] Homozygotes of $Cdk8^{K185}$ are third-instar-larval lethal. To avoid confounds from potential autosomal-recessive second-site mutations on the chromosome, we performed the rescue experiments in $Cdk8^{K185}$ *Cdk8 Df* flies that are also third-instar-larval lethal (Figure 2C). Using *actin-Gal4* to ubiquitously express fly *Cdk8* or human *CDK19* reference cDNA fully rescued the lethality of $Cdk8^{K185}$*/Df*, whereas expression of either CDK19 p.Tyr32His or p.Thr196Ala failed to rescue the lethality. These findings suggest that both CDK19 p.Tyr32His and CDK19 p.Thr196Ala are loss-of-function mutations (Figure 2C). Hence, both alleles correspond to dominant loss-of-function mutations.

CDK19 is known to be highly expressed in the nervous system.[19,21] We therefore performed a neuronal-specific knockdown by using two independent RNAi transgenes (*Cdk8 RNAi-1* and *Cdk8 RNAi-2*).[22] Both RNAis significantly reduce the level of *Cdk8* transcript to 5% (*RNAi-1*) or 10% (*RNAi-2*) of wild-type controls, respectively (Figure S1). All animals die as pupae by ubiquitous expression of *Cdk8 RNAi-1*. However, for *RNAi-2*, about 95% of the animals die at the pupal stage, but 5% of the flies eclose. These escapers can only live for ~5 days, but co-expression of the reference human *CDK19* fully rescued the pupal lethality and lifespan decrease (Figure 3A). However, co-expression of either variant (CDK19 p.Tyr32His or p.Thr196Ala) failed to rescue lethality (Figure 3A), again showing that these variants are pathogenic. We next examined whether *Cdk8* is required in neurons or glia. We knocked down *Cdk8* in neurons with the elav-Gal4 driver and in glia with the pan-glial driver repo-Gal4. Neuronal knockdown of *Cdk8* causes lethality, and only 7%–10% of flies eclose (Figure 3B), which is similar to the lethality observed with ubiquitous expression of *Cdk8 RNAi* (*da > Cdk8 RNAi*) (Figure 3A). However, glial knockdown of *Cdk8* via repo-gal4 does not cause lethality or other obvious behavioral defects (climbing or longevity), suggesting that *Cdk8* is required in neurons. The lethality observed upon neuronal knockdown is fully suppressed by co-expression of the human *CDK19* reference, but we observed no rescue when the variants were co-expressed (Figure 3B), suggesting that both *Cdk8* and *CDK19* share conserved function in the nervous system across species.

Given that all three probands exhibit medically refractory epilepsy, we performed "bang sensitivity" assays in flies. This assay can induce seizures in flies, as observed in potassium-channel mutants (*Shaker*) that have severe bang sensitivity and display seizure-like phenotypes.[23,24] Upon vortexing the flies for 10 s, normal flies right themselves within a few seconds, but flies that are sensitive to mechanical stress show stereotypical cycles of shaking and paralysis for many seconds and up to a minute.[25] These uncoordinated movements resemble seizures and have been documented to be suppressed by anti-convulsive drugs.[24] We found that neuronal knockdown of *Cdk8* results in very severe bang sensitivity in young flies (3 days old), and these flies need about ~45 s on average to recover from the vortex paradigm, whereas control flies recover in a few seconds (Figure 3C). Co-expression of the human reference *CDK19* fully suppressed the seizures, but co-expression of *CDK19* variants failed to rescue the bang-sensitivity defects (Figure 3C). In summary, loss of either *Cdk8* or *CDK19* is associated with severe seizures. Finally, neuronal knockdown of *Cdk8* (*elav > Cdk8 RNAi*; *UAS-lacZ*) decreases the lifespan of the escapers to ~10 days,

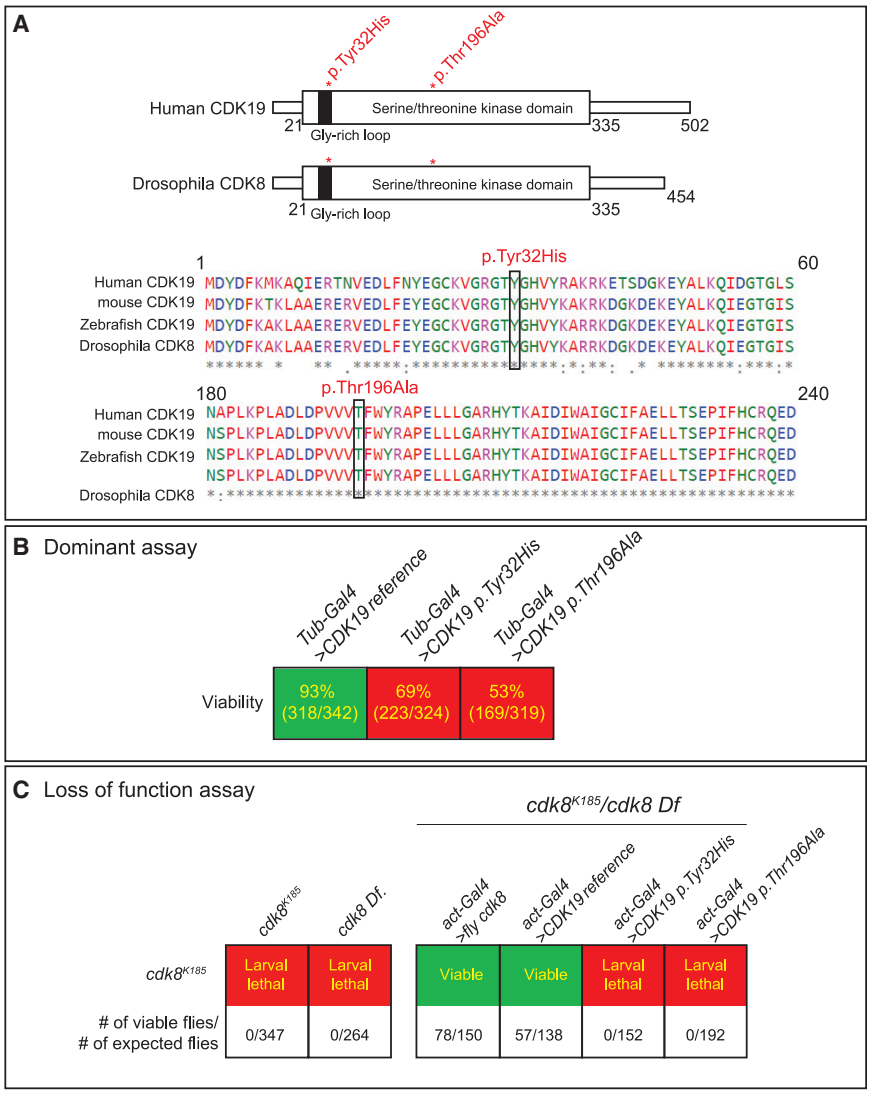

Figure 2. *Cdk8* Is Functional Fly Homolog of Human *CDK19*

(A) The domain that includes the variants is fully conserved from fly to human.

(B) Strong ubiquitous expression of *CDK19* reference is not toxic, but expression of the variants is toxic to flies. Numbers indicate the ratio of observed/expected flies.

(C) Ubiquitous expression of reference *CDK19* rescued the larval lethality observed in $Cdk8^{K185}$/*Cdk8 Df* flies, whereas the expression of variants *CDK19* failed to rescue the larval lethality. Numbers indicate the ratio of observed/expected flies.

whereas control flies live ~75 days (*elav* > *luciferase RNAi*). Again, this decrease in lifespan is fully restored by co-expression of reference *CDK19* but not by co-expression of *CDK19* variants.

To determine whether the subcellular localization of CDK19 is affected in the variants, we stained adult-fly CNS expressing the human reference CDK19 or variants in a background in which *Cdk8* is knocked down by RNAi. We find that both reference and variants are similarly expressed and that they are all localized to the perinuclear space and cytoplasm of most neurons in adult CNS (Figure 4 and Figure S2A). We also observed that both reference and variants are similarly localized to the nucleus in a few neurons in the adult CNS (Figures 4A–4B, white arrow), and larval CNS (Figure S2B). In summary, the variants do not affect the localization or abundance of CDK19, and the protein is localized to perinuclear cytoplasm.

Finally, to explore the consequences of the *CDK19* variants at synapses, we investigated the loss-of-function phenotypes at the larval *Drosophila* NMJ, a well-established model for synapse development and function.[26–29] We assessed the loss-of-function phenotypes of *Cdk8* at NMJs by expressing *Cdk8 RNAi* in neurons via the elav-Gal4 driver. As shown in Figure 5, we observed a significant decrease (~30%) in the total number of boutons, showing that loss of *Cdk8* affects synapse formation (Figures 5A and 5B). However, the number of branches is similar to the number in controls (Figure 5C). In summary, loss of *Cdk8* affects synapse development at NMJs.

Although *CDK8* and *CDK19* are very similar, several studies have documented that their functions are not redundant.[30,31] *CDK8* is known to be highly expressed in the bladder and esophagus, whereas *CDK19* is highly expressed in the brain.[14] Recently, *de novo* variants in *CDK8* have been linked to a syndromic neurodevelopmental disorder.[32]

Analyses of the Database of Genomic Variants (DGV) show that many individuals in the control population carry a deletion that encompasses the gene, indicating that loss of one copy of *CDK19* might not cause obvious clinical features. However, Mukhopadhyay et al.[30] reported a female individual who had a translocation disrupting the gene and who presented with bilateral congenital retinal folds, microcephaly, and mild intellectual disability. Finally, given that the pLI score for *CDK19* in the gnomAD database is 1, and the observed number of loss-of-function variants over expected loss-of-function variants is very low (observed versus expected, 0.03), *CDK19* is severely constrained for loss-of-function variation. This can be reconciled with our observations: ubiquitous overexpression of the human reference cDNA *CDK19* in a wild-type *Drosophila* background is not toxic, but expression of variants significantly reduced viability (Figure 2B), suggesting a dominant feature associated with the variants. We argue that this is a dominant-negative function because the two

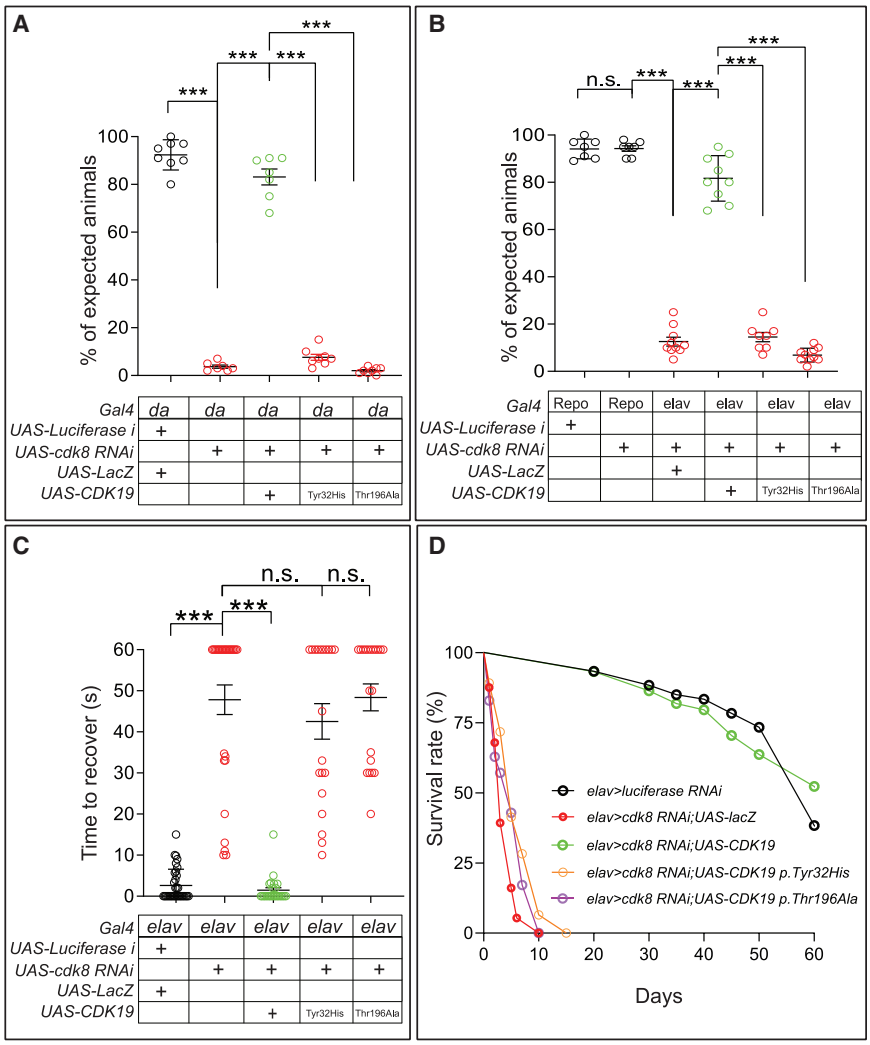

Figure 3. Loss of *Cdk8* Resulted in Lethality, Seizure, and Lifespan Decrease in Flies

(A) Ubiquitous expression of *Cdk8* RNAi caused lethality, and it can be rescued by co-expression of human reference *CDK19*, whereas it cannot be rescued by co-expression of *CDK19* variants (n = 8 crosses per each genotype). Statistical analyses were performed via one-way ANOVA followed by a Tukey post-hoc test. Results are means ± SEM, ***p < 0.001.

(B) Neuronal expression of *Cdk8 RNAi* caused severe lethality, but glial expression of *Cdk8 RNAi* did not cause any lethality. Co-expression of human reference *CDK19* rescued the lethality, whereas co-expression of *CDK19* variants failed to rescue the lethality (n = 9 crosses per each genotype). Statistical analyses were performed via one-way ANOVA followed by a Tukey post-hoc test. Results are means ± SEM, ***p < 0.001; n.s., not significant.

(C) Flies that lost *Cdk8* in neurons exhibit strong bang sensitivity, which can be fully rescued by expression of human reference CDK19, whereas they fail to be rescued by expression of the variants. Statistical analyses were performed via one-way ANOVA followed by a Tukey post-hoc test. Results are means ± SEM, ***p < 0.001; n.s., not significant.

(D) Lifespan of flies that co-express human reference CDK19 or the variants with *Cdk8 RNAi* (n > 50 per each genotype).

variants fail to rescue the lethality or neurologic phenotypes observed in the flies that lost *Cdk8* (Figures 2 and 3). Given that CDK19 interacts with mediator complex proteins, nonsynonymous variants in *CDK19* might cause dominant-negative effects.

In summary, we describe a syndrome associated with global developmental delay, hypotonia, dysmorphic features, and epilepsy in three individuals from three unrelated families harboring *de novo* missense variants in *CDK19*. On the basis of our experiments, we argue that *CDK19* plays a critical role in neurodevelopment and synapse formation and function, supporting the observation that it causes a neurodevelopmental syndrome with epilepsy in humans.

Supplemental Data

Supplemental Data can be found online at https://doi.org/10.1016/j.ajhg.2020.04.001.

Consortia

Members of the UDN include Maria T. Acosta, Margaret Adam, David R. Adams, Pankaj B. Agrawal, Mercedes E. Alejandro, Justin Alvey, Laura Amendola, Ashley Andrews, Euan A. Ashley, Mahshid S. Azamian, Carlos A. Bacino, Guney Bademci, Eva Baker, Ashok Balasubramanyam, Dustin Baldridge, Jim Bale, Michael Bamshad, Deborah Barbouth, Pinar Bayrak-Toydemir, Anita Beck, Alan H. Beggs, Edward Behrens, Gill Bejerano, Jimmy Bennet, Beverly Berg-Rood, Raphael Bernier, Jonathan A. Bernstein, Gerard T. Berry, Anna Bican, Stephanie Bivona, Elizabeth Blue, John Bohnsack, Carsten Bonnenmann, Devon Bonner, Lorenzo Botto, Brenna Boyd, Lauren C. Briere, Elly Brokamp, Gabrielle Brown, Elizabeth A. Burke, Lindsay C. Burrage, Manish J. Butte, Peter Byers, William E. Byrd, John Carey, Olveen Carrasquillo, Ta Chen Peter Chang, Sirisak Chanprasert, Hsiao-Tuan Chao, Gary D. Clark, Terra R. Coakley, Laurel A. Cobban, Joy D. Cogan, F. Sessions Cole, Heather A. Colley, Cynthia M. Cooper, Heidi Cope, William J. Craigen, Andrew B. Crouse, Michael Cunningham, Precilla D'Souza, Hongzheng Dai, Surendra Dasari, Mariska Davids, Jyoti G. Dayal, Matthew Deardorff, Esteban C. Dell'Angelica, Shweta U. Dhar, Katrina Dipple, Daniel Doherty, Naghmeh Dorrani, Emilie D. Douine, David D. Draper, Laura Duncan, Dawn Earl, David J. Eckstein, Lisa T. Emrick, Christine M. Eng, Cecilia Esteves, Tyra Estwick, Marni Falk, Liliana Fernandez, Carlos Ferreira, Elizabeth L. Fieg, Laurie C. Findley, Paul G. Fisher, Brent L. Fogel, Irman Forghani, Laure Fresard, William A. Gahl, Ian Glass, Rena A. Godfrey, Katie Golden-Grant, Alica M. Goldman, David B. Goldstein, Alana Grajewski, Catherine A. Groden, Andrea L. Gropman, Irma Gutierrez, Sihoun Hahn,

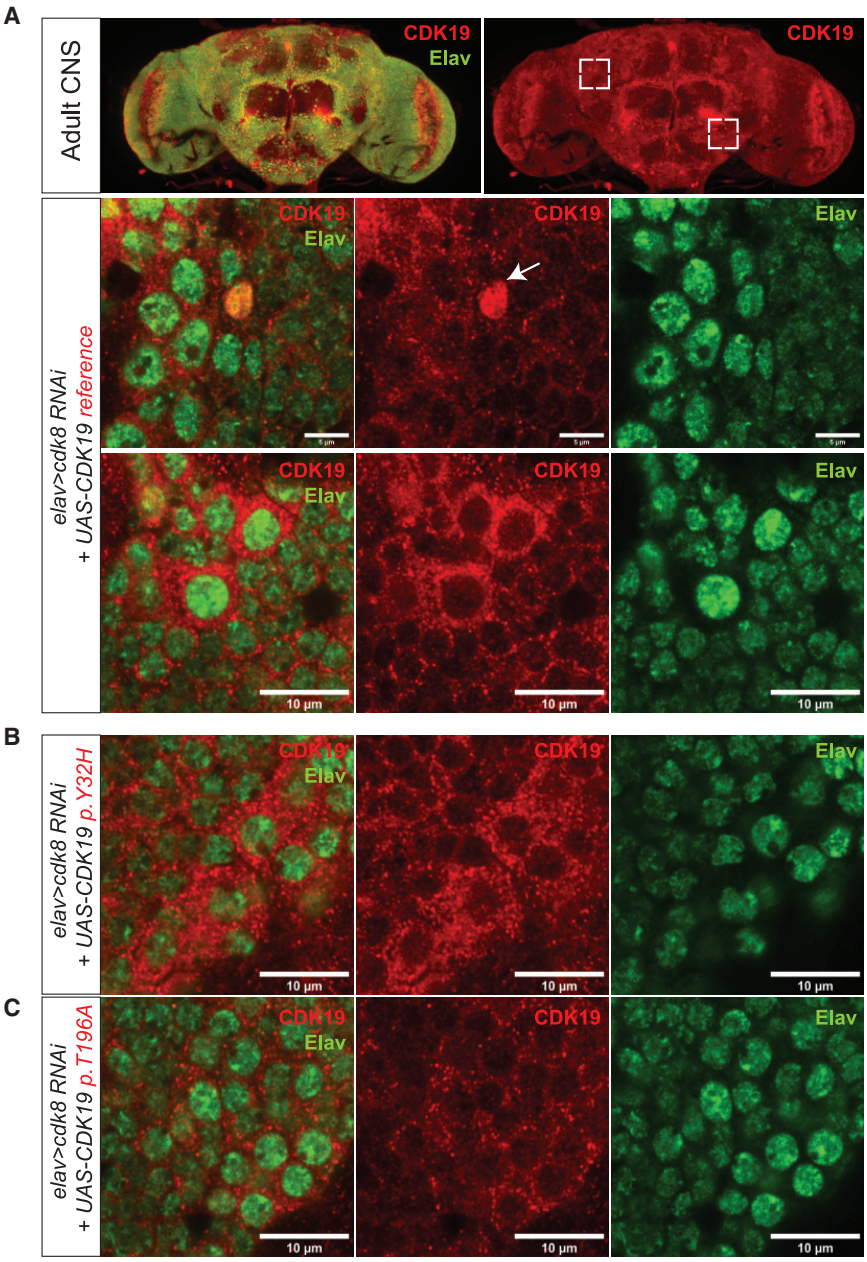

Figure 4. CDK19 Is Localized to the Perinuclear Space and Cytoplasm of Most Neurons but Expressed in the Nucleus in a Few Neurons

(A) Localization of CDK19 in humanized flies (*elav > Cdk8 RNAi; UAS-CDK19 reference*). Dashed boxes indicate the region that are magnified in images below. White arrow indicates the neuron that expresses CDK19 in nucleus. Scale bar: 10 µm.

(B) Localization of variant CDK19 in the flies (*elav > Cdk8 RNAi; UAS-CDK19 p.Thr196Ala*).

(C) Localization of variant CDK19 in the flies (*elav > Cdk8 RNAi; UAS-CDK19 p.Tyr32His*). Scale bar: 10 µm.

Rizwan Hamid, Neil A. Hanchard, Kelly Hassey, Nichole Hayes, Frances High, Anne Hing, Fuki M. Hisama, Ingrid A. Holm, Jason Hom, Martha Horike-Pyne, Alden Huang, Yong Huang, Rosario Isasi, Fariha Jamal, Gail P. Jarvik, Jeffrey Jarvik, Suman Jayadev, Jean M. Johnston, Lefkothea Karaviti, Emily G. Kelley, Jennifer Kennedy, Dana Kiley, Isaac S. Kohane, Jennefer N. Kohler, Deborah Krakow, Donna M. Krasnewich, Elijah Kravets, Susan Korrick, Mary Koziura, Joel B. Krier, Seema R. Lalani, Byron Lam, Christina Lam, Brendan C. Lanpher, Ian R. Lanza, C. Christopher Lau, Kimberly LeBlanc, Brendan H. Lee, Hane Lee, Roy Levitt, Richard A. Lewis, Sharyn A. Lincoln, Pengfei Liu, Xue Zhong Liu, Nicola Longo, Sandra K. Loo, Joseph Loscalzo, Richard L. Maas, Ellen F. Macnamara, Calum A. MacRae, Valerie V. Maduro, Marta M. Majcherska, May Christine V. Malicdan, Laura A. Mamounas, Teri A. Manolio, Rong Mao, Kenneth Maravilla, Thomas C. Markello, Ronit Marom, Gabor Marth, Beth A. Martin, Martin G. Martin, Julian A. Martínez-Agosto, Shruti Marwaha, Jacob McCauley, Allyn McConkie-Rosell, Colleen E. McCormack, Alexa T. McCray, Elisabeth McGee, Heather Mefford, J. Lawrence Merritt, Matthew Might, Ghayda Mirzaa, Eva Morava, Paolo M. Moretti, Marie Morimoto, John J. Mulvihill, David R. Murdock, Mariko Nakano-Okuno, Avi Nath, Stan F. Nelson, John H. Newman, Sarah K. Nicholas, Deborah Nickerson, Donna Novacic, Devin Oglesbee, James P. Orengo, Laura Pace, Stephen Pak, J. Carl Pallais, Christina GS. Palmer, Jeanette C. Papp, Neil H. Parker, John A. Phillips III, Jennifer E. Posey, Lorraine Potocki, Barbara N. Pusey, Aaron Quinlan, Wendy Raskind, Archana N. Raja, Genecee Renteria, Chloe M. Reuter, Lynette Rives, Amy K. Robertson, Lance H. Rodan, Jill A. Rosenfeld, Natalie Rosenwasser, Maura Ruzhnikov, Ralph Sacco, Jacinda B. Sampson, Susan L. Samson, Mario Saporta, C. Ron Scott, Judy Schaechter, Timothy Schedl, Kelly Schoch, Daryl A. Scott, Prashant Sharma, Vandana Shashi, Jimann Shin, Rebecca Signer, Catherine H. Sillari, Edwin K. Silverman, Janet S. Sinsheimer, Kathy Sisco, Edward C. Smith, Kevin S. Smith, Emily Solem, Lilianna Solnica-Krezel, Rebecca C. Spillmann, Joan M. Stoler, Nicholas Stong, Jennifer A. Sullivan, Kathleen Sullivan, Angela Sun, Shirley Sutton, David A. Sweetser, Virginia Sybert, Holly K. Tabor, Cecelia P. Tamburro, Queenie K.-G. Tan, Mustafa Tekin, Fred Telischi, Willa Thorson, Cynthia J. Tifft, Camilo Toro, Alyssa A. Tran, Brianna M. Tucker, Tiina K. Urv, Adeline Vanderver, Matt Velinder, Dave Viskochil, Tiphanie P. Vogel, Colleen E. Wahl, Stephanie Wallace, Nicole M. Walley, Chris A. Walsh, Melissa Walker, Jennifer Wambach, Jijun Wan, Lee-kai Wang, Michael F. Wangler, Patricia A. Ward, Daniel Wegner, Mark Wener, Tara Wenger, Katherine Wesseling Perry, Monte Westerfield, Matthew T. Wheeler, Jordan Whitlock, Lynne A. Wolfe, Jeremy D. Woods, Shinya Yamamoto, John Yang, Guoyun Yu, Diane B. Zastrow, Chunli Zhao, Stephan Zuchner.

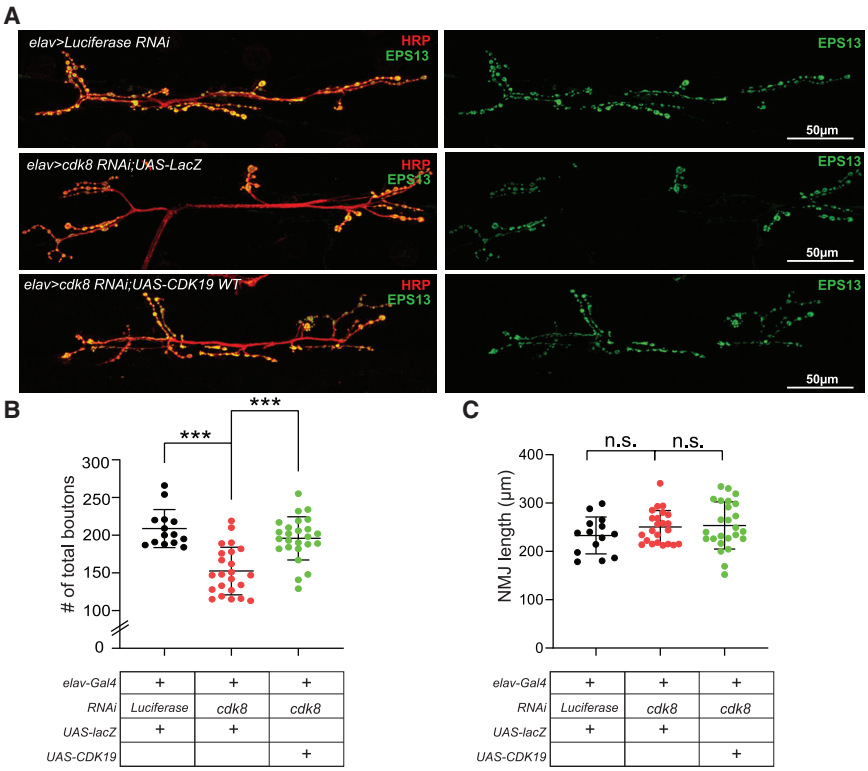

Figure 5. Loss of *Cdk8* Caused a Severe Synapse Loss in Larval NMJs

(A) Representative images of larval NMJs of each genotype (Control, *elav > luciferase RNAi* [top]; *Cdk8* loss, *elav > Cdk8 RNAi;UAS-LacZ* [middle]; and rescued flies, *elav > Cdk8 RNAi;UAS-CDK19 reference* [bottom]).

(B) Quantification of the number of total boutons in NMJs (n = 14 [control], n = 23 [*Cdk8* loss], n = 25 [rescued flies]). Statistical analyses were performed via one-way ANOVA followed by a Tukey post-hoc test. Results are means ± SEM, ***$p < 0.001$.

(C) Quantification of the length of boutons of NMJs (n = 14 [control], n = 23 [*Cdk8* loss], n = 25 [rescued flies]). Statistical analyses were performed via one-way ANOVA followed by a Tukey post-hoc test. Results are means ± SEM, n.s., not significant.

Acknowledgments

We would like to thank the affected individuals and families who participated in this study. Research reported in this manuscript was supported by the NIH Common Fund, through the Office of Strategic Coordination and Office of the NIH Director under Award Numbers U01HG007709 (BCM clinical site) and U01HG007942 (BCM sequencing core). The content is solely the responsibility of the authors and does not necessarily represent the official views of the NIH. H.J.B. is supported by NIH grant number U54 from NINDS R24OD022005 and is an investigator of the Howard Hughes Medical Institute. X.M., H.W., and B.X. are supported by Hunan Provincial Major Science and Technology Project (grant number 2019SK1010), National Natural Science Foundation of China (grant number 81974206), and National Natural Science Foundation of China (grant number 81801136). The confocal microscopy facility at the Neurological Research Institute is a part of Neurovisualization Core of the Intellectual and Developmental Disabilities Research Center (IDDRC) supported by NIH U54HD083092. P.C.M. is supported by CIHR (MFE-164712). C.A.B., J.A.R., L.B., P.L., D.R.M., and H.T.C. are supported in part by NIH grant U01HG007709. H.T.C.'s research effort is supported in part by the American Academy of Neurology, Child Neurology Foundation, Burroughs Wellcome Fund, and the McNair Medical Institute at the Robert and Janice McNair Foundation.

Declaration of Interests

The Department of Molecular and Human Genetics at Baylor College of Medicine receives revenue from clinical genetic testing completed at Baylor Genetics Laboratories. The authors declare no other competing interests.

Received: February 20, 2020
Accepted: March 30, 2020
Published: April 23, 2020

Web Resources

CADD, https://cadd.gs.washington.edu/
DECIPHER, https://decipher.sanger.ac.uk/
gnomAD, http://gnomad.broadinstitute.org/
MARRVEL, http://www.marrvel.org/
OMIM, http://www.omim.org/
PolyPhen-2, http://genetics.bwh.harvard.edu/pph2/
PROVEAN, http://provean.jcvi.org/
SIFT, https://sift.bii.a-star.edu.sg/
Undiagnosed Diseases Network, https://undiagnosed.hms.harvard.edu

References

1. Hrachovy, R.A. (2002). West's syndrome (infantile spasms). Clinical description and diagnosis. Adv. Exp. Med. Biol. *497*, 33–50.
2. Hongou, K., Konishi, T., Yagi, S., Araki, K., and Miyawaki, T. (1998). Rotavirus encephalitis mimicking afebrile benign convulsions in infants. Pediatr. Neurol. *18*, 354–357.
3. Hayashi, M., Itoh, M., Araki, S., Kumada, S., Tanuma, N., Kohji, T., Kohyama, J., Iwakawa, Y., Satoh, J., and Morimatsu, Y. (2000). Immunohistochemical analysis of brainstem lesions in infantile spasms. Neuropathology *20*, 297–303.
4. O'Callaghan, F.J., Harris, T., Joinson, C., Bolton, P., Noakes, M., Presdee, D., Renowden, S., Shiell, A., Martyn, C.N., and Osborne, J.P. (2004). The relation of infantile spasms, tubers,

and intelligence in tuberous sclerosis complex. Arch. Dis. Child. *89*, 530–533.
5. Paciorkowski, A.R., Thio, L.L., and Dobyns, W.B. (2011). Genetic and biologic classification of infantile spasms. Pediatr. Neurol. *45*, 355–367.
6. Appleton, R.E. (2001). West syndrome: long-term prognosis and social aspects. Brain Dev. *23*, 688–691.
7. Galbraith, M.D., Donner, A.J., and Espinosa, J.M. (2010). CDK8: a positive regulator of transcription. Transcription *1*, 4–12.
8. Bourbon, H.M. (2008). Comparative genomics supports a deep evolutionary origin for the large, four-module transcriptional mediator complex. Nucleic Acids Res. *36*, 3993–4008.
9. Risheg, H., Graham, J.M., Jr., Clark, R.D., Rogers, R.C., Opitz, J.M., Moeschler, J.B., Peiffer, A.P., May, M., Joseph, S.M., Jones, J.R., et al. (2007). A recurrent mutation in MED12 leading to R961W causes Opitz-Kaveggia syndrome. Nat. Genet. *39*, 451–453.
10. Asadollahi, R., Oneda, B., Sheth, F., Azzarello-Burri, S., Baldinger, R., Joset, P., Latal, B., Knirsch, W., Desai, S., Baumer, A., et al. (2013). Dosage changes of MED13L further delineate its role in congenital heart defects and intellectual disability. Eur. J. Hum. Genet. *21*, 1100–1104.
11. Firestein, R., Bass, A.J., Kim, S.Y., Dunn, I.F., Silver, S.J., Guney, I., Freed, E., Ligon, A.H., Vena, N., Ogino, S., et al. (2008). CDK8 is a colorectal cancer oncogene that regulates beta-catenin activity. Nature *455*, 547–551.
12. Pelish, H.E., Liau, B.B., Nitulescu, I.I., Tangpeerachaikul, A., Poss, Z.C., Da Silva, D.H., Caruso, B.T., Arefolov, A., Fadeyi, O., Christie, A.L., et al. (2015). Mediator kinase inhibition further activates super-enhancer-associated genes in AML. Nature *526*, 273–276.
13. Sato, S., Tomomori-Sato, C., Parmely, T.J., Florens, L., Zybailov, B., Swanson, S.K., Banks, C.A., Jin, J., Cai, Y., Washburn, M.P., et al. (2004). A set of consensus mammalian mediator subunits identified by multidimensional protein identification technology. Mol. Cell *14*, 685–691.
14. Galbraith, M.D., Allen, M.A., Bensard, C.L., Wang, X., Schwinn, M.K., Qin, B., Long, H.W., Daniels, D.L., Hahn, W.C., Dowell, R.D., and Espinosa, J.M. (2013). HIF1A employs CDK8-mediator to stimulate RNAPII elongation in response to hypoxia. Cell *153*, 1327–1339.
15. Westerling, T., Kuuluvainen, E., and Mäkelä, T.P. (2007). Cdk8 is essential for preimplantation mouse development. Mol. Cell. Biol. *27*, 6177–6182.
16. Brown, S.D., and Moore, M.W. (2012). The International Mouse Phenotyping Consortium: past and future perspectives on mouse phenotyping. Mamm. Genome *23*, 632–640.
17. Karczewski, K.J., Francioli, L.C., Tiao, G., Cummings, B.B., Alföldi, J., Wang, Q., Collins, R.L., Laricchia, K.M., Ganna, A., Birnbaum, D.P., et al. (2019). Variation across 141,456 human exomes and genomes reveals the spectrum of loss-offunction intolerance across human protein-coding genes. bioRxiv.
18. Hu, Y., Flockhart, I., Vinayagam, A., Bergwitz, C., Berger, B., Perrimon, N., and Mohr, S.E. (2011). An integrative approach to ortholog prediction for disease-focused and other functional studies. BMC Bioinformatics *12*, 357.
19. Wang, J., Al-Ouran, R., Hu, Y., Kim, S.Y., Wan, Y.W., Wangler, M.F., Yamamoto, S., Chao, H.T., Comjean, A., Mohr, S.E., et al.; UDN (2017). MARRVEL: Integration of Human and Model Organism Genetic Resources to Facilitate Functional Annotation of the Human Genome. Am. J. Hum. Genet. *100*, 843–853.
20. Loncle, N., Boube, M., Joulia, L., Boschiero, C., Werner, M., Cribbs, D.L., and Bourbon, H.M. (2007). Distinct roles for Mediator Cdk8 module subunits in Drosophila development. EMBO J. *26*, 1045–1054.
21. Davie, K., Janssens, J., Koldere, D., De Waegeneer, M., Pech, U., Kreft, L., Aibar, S., Makhzami, S., Christiaens, V., Bravo Gonzalez-Blas, C., et al. (2018). A Single-Cell Transcriptome Atlas of the Aging Drosophila Brain. Cell *174*, 982–998.
22. Ni, J.Q., Zhou, R., Czech, B., Liu, L.P., Holderbaum, L., Yang-Zhou, D., Shim, H.S., Tao, R., Handler, D., Karpowicz, P., et al. (2011). A genome-scale shRNA resource for transgenic RNAi in Drosophila. Nat. Methods *8*, 405–407.
23. Kuebler, D., and Tanouye, M.A. (2000). Modifications of seizure susceptibility in Drosophila. J. Neurophysiol. *83*, 998–1009.
24. Parker, L., Howlett, I.C., Rusan, Z.M., and Tanouye, M.A. (2011). Seizure and epilepsy: studies of seizure disorders in Drosophila. Int. Rev. Neurobiol. *99*, 1–21.
25. Kanca, O., Andrews, J.C., Lee, P.T., Patel, C., Braddock, S.R., Slavotinek, A.M., Cohen, J.S., Gubbels, C.S., Aldinger, K.A., Williams, J., et al.; Undiagnosed Diseases Network (2019). De Novo Variants in WDR37 Are Associated with Epilepsy, Colobomas, Dysmorphism, Developmental Delay, Intellectual Disability, and Cerebellar Hypoplasia. Am. J. Hum. Genet. *105*, 672–674.
26. Menon, K.P., Carrillo, R.A., and Zinn, K. (2013). Development and plasticity of the Drosophila larval neuromuscular junction. Wiley Interdiscip. Rev. Dev. Biol. *2*, 647–670.
27. Verstreken, P., Ly, C.V., Venken, K.J., Koh, T.W., Zhou, Y., and Bellen, H.J. (2005). Synaptic mitochondria are critical for mobilization of reserve pool vesicles at Drosophila neuromuscular junctions. Neuron *47*, 365–378.
28. Estes, P.S., Daniel, S.G., McCallum, A.P., Boehringer, A.V., Sukhina, A.S., Zwick, R.A., and Zarnescu, D.C. (2013). Motor neurons and glia exhibit specific individualized responses to TDP-43 expression in a Drosophila model of amyotrophic lateral sclerosis. Dis. Model. Mech. *6*, 721–733.
29. Mhatre, S.D., Michelson, S.J., Gomes, J., Tabb, L.P., Saunders, A.J., and Marenda, D.R. (2014). Development and characterization of an aged onset model of Alzheimer's disease in Drosophila melanogaster. Exp. Neurol. *261*, 772–781.
30. Mukhopadhyay, A., Kramer, J.M., Merkx, G., Lugtenberg, D., Smeets, D.F., Oortveld, M.A., Blokland, E.A., Agrawal, J., Schenck, A., van Bokhoven, H., et al. (2010). CDK19 is disrupted in a female patient with bilateral congenital retinal folds, microcephaly and mild mental retardation. Hum. Genet. *128*, 281–291.
31. Tsutsui, T., Umemura, H., Tanaka, A., Mizuki, F., Hirose, Y., and Ohkuma, Y. (2008). Human mediator kinase subunit CDK11 plays a negative role in viral activator VP16-dependent transcriptional regulation. Genes Cells *13*, 817–826.
32. Calpena, E., Hervieu, A., Kaserer, T., Swagemakers, S.M.A., Goos, J.A.C., Popoola, O., Ortiz-Ruiz, M.J., Barbaro-Dieber, T., Bownass, L., Brilstra, E.H., et al.; Deciphering Developmental Disorders Study (2019). De Novo Missense Substitutions in the Gene Encoding CDK8, a Regulator of the Mediator Complex, Cause a Syndromic Developmental Disorder. Am. J. Hum. Genet. *104*, 709–720.

The American Journal of Human Genetics, Volume *106*

Supplemental Data

De Novo Variants in *CDK19* Are Associated with a Syndrome Involving Intellectual Disability and Epileptic Encephalopathy

Hyung-lok Chung, Xiao Mao, Hua Wang, Ye-Jin Park, Paul C. Marcogliese, Jill A. Rosenfeld, Lindsay C. Burrage, Pengfei Liu, David R. Murdock, Shinya Yamamoto, Michael F. Wangler, Undiagnosed Diseases Network, Hsiao-Tuan Chao, Hongyu Long, Li Feng, Carlos A. Bacino, Hugo J. Bellen, and Bo Xiao

SUPPLEMENTAL DATA

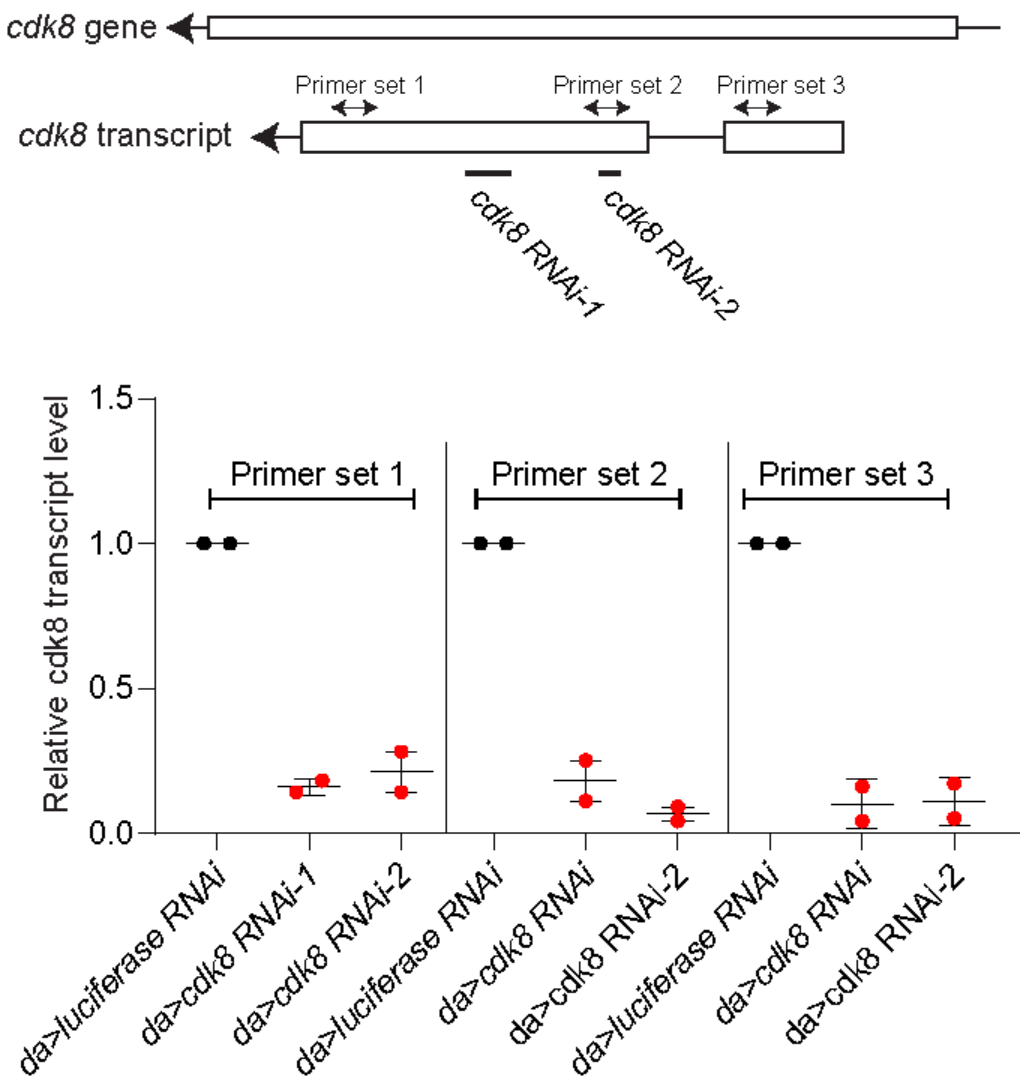

Figure S1: Two independent RNAis can efficiently reduce the transcripts level.

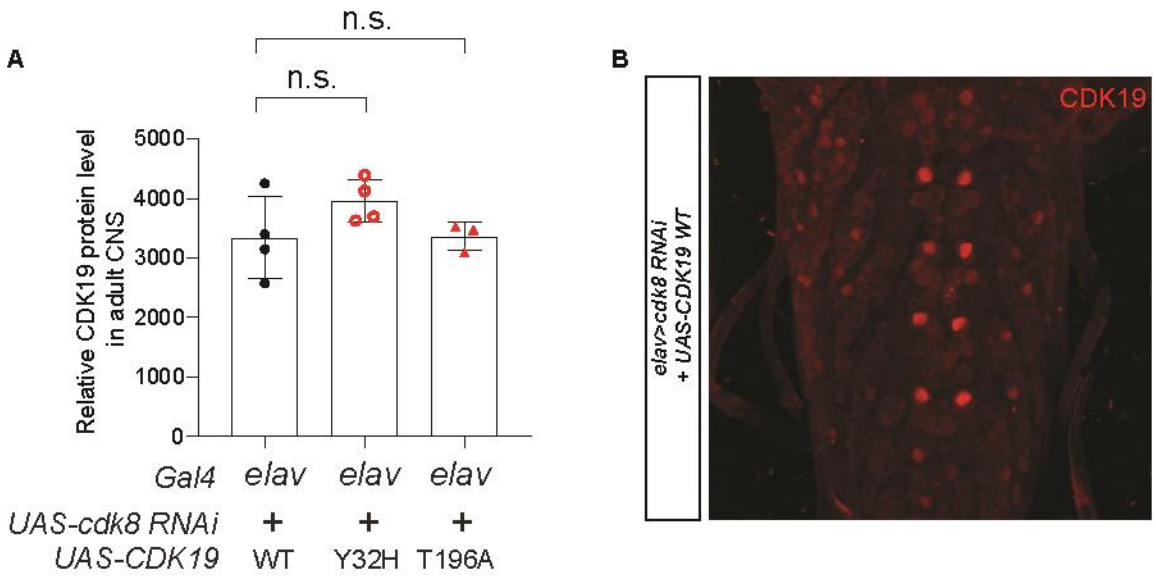

Figure S2: *CDK19* reference and variants are similarly expressed in CNS of flies.

(A) The relative intensity of CDK19 signal in adult fly CNS is comparable when we overexpressed the CDK19 reference or CDK19 variants (n = 4 for CDK19 reference, n = 4 for CDK19 p. Tyr32His and n = 3 for CDK19 p. Thr196Ala). Statistical analyses are one-way ANOVA followed by a Tukey post-hoc test. Results are mean ± s.e.m; n.s., not significant.

Supplemental Materials and Methods

Informed consent

Informed consent was obtained from the parents of proband 1 for participation in the Undiagnosed Diseases Network study at Baylor College of Medicine. This protocol has been approved under the oversight of the National Institutes of Health Institutional Review Board. Additionally, informed consent was obtained for publication of photos shown here. Patient 2 and 3 were recruited to the Xiangya hospital Epilepsy Cohort which aims to elucidate the genetic basis

of epilepsy and epilepsy related developmental disease. Patients were recruited to the study during 2018 to 2019. Both of them underwent detailed medical history collection and physical examination by neurologists. DNA was extracted from peripheral venous blood using the Genomic DNA kit from Aidlab. This study was approved by the Ethics Committee of Xiangya hospital, Central South University (No.201605577). Informed consents were obtained from both enrolled participants for publication of photos shown here.

Genetic analysis

Trio whole genome sequencing (WGS) was performed for proband 1 at Baylor Genetics (BG) as part of the Undiagnosed Diseases Network (UDN). The library is prepared using a PCR free 550-bp insert size protocol by the KAPA Hyper Prep kit. The library is subjected to sequence analysis on Illumina NovaSeq 6000 platform for 150 bp paired-end reads. The following quality control metrics of the sequencing data are generally achieved: average sequenced coverage over the genome > 40X, >97.5% target base (digital exome) covered at >20X, SNP concordance to genotype array: >95%. BG WGS data were aligned to the hg38 reference sequence on the Illumina Dragen pipeline. For compatibility with the BCM UDN annotation pipeline based on the Codified Genomics (Houston, TX) interpretation tool, the BAM files were first converted back to FASTQ files and then realigned to the hg19 reference. Variant calling was then performed on the realigned BAM files and subsequent VCFs were annotated. We filtered for rare variants that had a frequency of <0.01 in gnomAD (https://gnomad.broadinstitute.org/) and in our local database which consists of over 750 samples. For our initial analysis, we focused on *de novo* variants, and genes with biallelic variants where at least one variant was in the coding region or at a canonical splice site.

Trio ES of probands 2 and 3 was performed using the HiSeq2500 system (Illumina, San Diego, CA, USA) with a mean depth of 100X. The ES data was analyzed by using a customized pipeline,[32]

and ANNOVAR software was used to annotate the data[33]. Public databases (ESP6500, 1000genomes, ExAC, gnomAD) were used to filter variants with frequencies higher than 0.001. Variants in exonic regions and splicing regions were remained after removing variants in UTR regions, non-coding regions and intronic regions. Synonymous variants were also filtered. Sanger sequencing was used to validate trio ES results. A *de novo* variant in *EFCAB13 (c.583C>G)* and compound heterozygous variants in *ADGRE1* (*c.587C>T, c.662G>A*) were additionally identified, however, all these 3 variants were predicted to be tolerable or not conserved.

A *de novo* variant in WDR63 (c.449A>G) was identified in proband 3, however this variant was predicted to be tolerable or not conserved. We also identified compound heterozygous variants in *CEP164* (*c.548T>A, c.3965C>T*) and *PKD1* (*c.191G>C, c.4343C>T*). All the four variants were predicted to be tolerable, and the patient 3 showed no clinical features to related the diseases related to *CEP164* or *PKD1* (Nephronophthisis (*CEP164*, OMIM #614845) and polycystic kidney disease (*PKD1*, OMIM #173900)).

Drosophila **genetics**

The following stocks were obtained from the Bloomington *Drosophila* Stock Center (BDSC) at Indiana University: y^1 *w*; P {Act5C-GAL4} 25FO1/CyO, y+* (RRID: BDSC_4414[34]), *w[*];da-GAL4* (RRID : BDSC_5460), *w[1118]; P{GAL4}repo/TM3, Sb1* (RRID: BDSC_7415), *P{GAL4-elav.L}2/CyO* (RRID: BDSC_8765[35]), y^1 sc^* v^1 sev^{21}*; P{TRiP.GL00231}attP2* (RRID: BDSC_35324[22]), y^1 *sc* v*^{1} sev^{21}*;* P{TRiP.HMS05476}attP40 (RRID: BDSC_67010;[22]).

Generation of ***CDK19 Drosophila*** **transgenes**

UAS-CDK19 reference and variant transgenic flies were generated as previously described[36; 37].

Using Gateway cloning (Thermo Fisher Scientific), the *CDK19* cDNA entry clone (GenBank: NM_015076.3) in the pDONR221 vector was shuttled to the pGW-attB-HA[38]. Site-directed mutagenesis was performed with the Q5 site-directed mutagenesis kit (NEB) followed by Sanger verification. The following forward and reverse primers were used to make *CDK19* variants:

CDK19 p. Y32H: FW- ACGCGGCACCCACGGTCACGT,

RV- CCCACTTTGCACCCTTCGTACTC

CDK19 p. T196A: FW- AGTAGTTGTGGCATTTTGGTATC,

RV- GGATCCAAATCTGCTAGTG

All UAS-cDNA Constructs were inserted into the VK37 (PBac{y[+]-attP}VK00037) docking site by ϕC31 mediated transgenesis[39].

Quantitative real-time PCR

Total RNA was extracted from adult flies using RNeasy Plus Mini Kit (QIAGEN) and 1.5 µg RNA was reverse transcribed to synthesize cDNA using a 5X All-In-One RT MasterMix (abm). qPCR was performed with iTaq Universal SYBR Green Supermix (BIO-RAD) and CFX96 Touch Real-Time PCR Detection System (BIO-RAD). The level of Rp49 transcripts was used for normalization.

The following primers were used for PCR:

Rp49 FW (5′- ACAGGCCCAAGATCGTGAAGA -3′)

Rp49-RV (5′- CGCACTCTGTTGTCGATACCCT-3′)

Cdk8-1-FW (5′- CCAGCAAGATTTTCACCACCA -3′)

Cdk8-1-RV (5′- CAGTTGAAGCGCTGGAAGTTCT -3′)

Cdk8-2-FW (5′- CATCCGGGTGTTTCTGTCG -3′)

Cdk8-2-RV (5′- CAGCCCGATGGAACTTAATGAT-3′)

Cdk8-3-FW (5′- GTCTACAAGGCGAAATGGAAGG -3′)

Cdk8-3-RV (5′- CGGACATGGACAATCCGGTG -3′)

Immunohistochemistry of adult fly brains

Fly brains were dissected in cold 1X PBS, and were fixed with 4% paraformaldehyde for 30 minutes at room temperature (RT). Tissues were washed in PBST solution (1X PBS, 0.1%Triton X-100) and incubated with 5% NGS (Normal Goat Serum) at room temperature (RT) for 2 hours and incubated with primary antibodies with 5% NGS solution on a rotating platform overnight at 4°C. The brains were washed again with PBST prior to incubation with secondary antibodies on a rotating platform overnight at 4°C in the dark and thoroughly rinsed in PBST and mounted with Vectashield for imaging. Leica SP8X Confocal Microscope was used for imaging.

Primary antibodies used in this study were as follows: Mouse anti-Elav (9F8A9, 1:50, DSHB) and Rabbit anti-CDK19 (SAB4301196, 1:200, Sigma-aldrich). For secondary antibodies, goat anti-mouse-IgG with Alexa Fluor 488 and anti-rabbit Cy5 (Jackson ImmunoResearch) were used.

Dissecting and staining for larval NMJ.

NMJs were dissected and fixed from wandering third instar larvae, as described previously[40]. The tissues were incubated with 5% Normal Goat Serum solution for blocking at RT for 2 hours and then incubated with primary antibodies with 5% NGS solution on a rotating platform overnight at 4°C. The tissues were washed again with PBST before incubation with secondary antibodies on a rotating platform overnight at 4°C in the dark and then thoroughly rinsed in PBST and mounted with Vectashield for imaging. The NMJs between muscles 6/7 of the A3 segment were imaged by

Leica SP8 X Confocal Microscope. ImageJ was used for quantification of boutons, branches, and NMJ length. Synaptic branches with two or more synaptic boutons were considered branches, according to Miller et al., 2012[41].

Supplemental references

37. Ansar, M., Chung, H.L., Al-Otaibi, A., Elagabani, M.N., Ravenscroft, T.A., Paracha, S.A., Scholz, R., Abdel Magid, T., Sarwar, M.T., Shah, S.F., et al. (2019). Bi-allelic Variants in IQSEC1 Cause Intellectual Disability, Developmental Delay, and Short Stature. Am J Hum Genet. 105, 907.
38. Bischof, J., Bjorklund, M., Furger, E., Schertel, C., Taipale, J., and Basler, K. (2013). A versatile platform for creating a comprehensive UAS-ORFeome library in Drosophila. Development 140, 2434-2442.
39. Venken, K.J., He, Y., Hoskins, R.A., and Bellen, H.J. (2006). P[acman]: a BAC transgenic platform for targeted insertion of large DNA fragments in D. melanogaster. Science 314, 1747-1751.
40. Smith, R., and Taylor, J.P. (2011). Dissection and imaging of active zones in the Drosophila neuromuscular junction. J Vis Exp.
41. Miller, D.L., Ballard, S.L., and Ganetzky, B. (2012). Analysis of synaptic growth and function in Drosophila with an extended larval stage. J Neurosci 32, 13776-13786.